

## Experiment Report Form

The double page inside this form is to be filled in by all users or groups of users who have had access to beam time for measurements at the ESRF.

Once completed, the report should be submitted electronically to the User Office via the User Portal:  
<https://www.esrf.fr/misapps/SMISWebClient/protected/welcome.do>

### Deadlines for submission of Experimental Reports

Experimental reports must be submitted within the period of 3 months after the end of the experiment.

#### Experiment Report supporting a new proposal (“relevant report”)

If you are submitting a proposal for a new project, or to continue a project for which you have previously been allocated beam time, you must submit a report on each of your previous measurement(s):

- even on those carried out close to the proposal submission deadline (it can be a “*preliminary report*”),
- even for experiments whose scientific area is different from the scientific area of the new proposal,
- carried out on CRG beamlines.

You must then register the report(s) as “relevant report(s)” in the new application form for beam time.

### Deadlines for submitting a report supporting a new proposal

- 1<sup>st</sup> March Proposal Round - **5<sup>th</sup> March**
- 10<sup>th</sup> September Proposal Round - **13<sup>th</sup> September**

The Review Committees reserve the right to reject new proposals from groups who have not reported on the use of beam time allocated previously.

#### Reports on experiments relating to long term projects

Proposers awarded beam time for a long term project are required to submit an interim report at the end of each year, irrespective of the number of shifts of beam time they have used.

#### Published papers

All users must give proper credit to ESRF staff members and proper mention to ESRF facilities which were essential for the results described in any ensuing publication. Further, they are obliged to send to the Joint ESRF/ ILL library the complete reference and the abstract of all papers appearing in print, and resulting from the use of the ESRF.

Should you wish to make more general comments on the experiment, please note them on the User Evaluation Form, and send both the Report and the Evaluation Form to the User Office.

### Instructions for preparing your Report

- fill in a separate form for each project or series of measurements.
- type your report in English.
- include the experiment number to which the report refers.
- make sure that the text, tables and figures fit into the space available.
- if your work is published or is in press, you may prefer to paste in the abstract, and add full reference details. If the abstract is in a language other than English, please include an English translation.



<b>Experiment title:</b> Polymer crystallization on nano-curved surfaces		<b>Experiment number:</b> <b>SC 5060</b>
<b>Beamline:</b>	<b>Date of experiment:</b> from: 02/09/2020 to: 08/09/2020 from: 29/10/2020 to: 31/10/2020	<b>Date of report:</b>
<b>Shifts:</b> 18	<b>Local contact(s):</b> Oleg Konovalov and Maciej Jankowski	<i>Received at ESRF:</i>
<b>Names and affiliations of applicants (* indicates experimentalists):</b> Roberta Ruffino, Giovanni Calogero Li Destri Nicosia, Nunzio Tuccitto and Luca Fichera		

**Report:** The goal of the project was the determination of the effect of substrate nanoscale-curvature and surface free energy (SFE) on the crystallization behaviour of a model semi-crystalline polymer, namely poly-3-hexylthiophene, ultrathin films by combined GID and GISAXS. In particular we have performed the structural characterization of as-prepared (out of equilibrium), *ex-situ* and *in-situ* thermally annealed films deposited on flat and nano-curved substrates, consisting of nanoparticle monolayers deposited on a flat substrate. ID 10 beamline perfectly fitted to our experimental plans thanks to the possibility to easily switch from GISAXS to GID configuration and the sufficiently long sample-to-detector distance enabling the determination of the low- $q$  GISAXS signals. Sample thermal annealing was performed in-vacuum with excellent temperature control, however, very special care was to put on the vacuum inside the sample chamber since, from time-to-time, we observed significant sample oxidation caused by residual oxygen in the chamber.

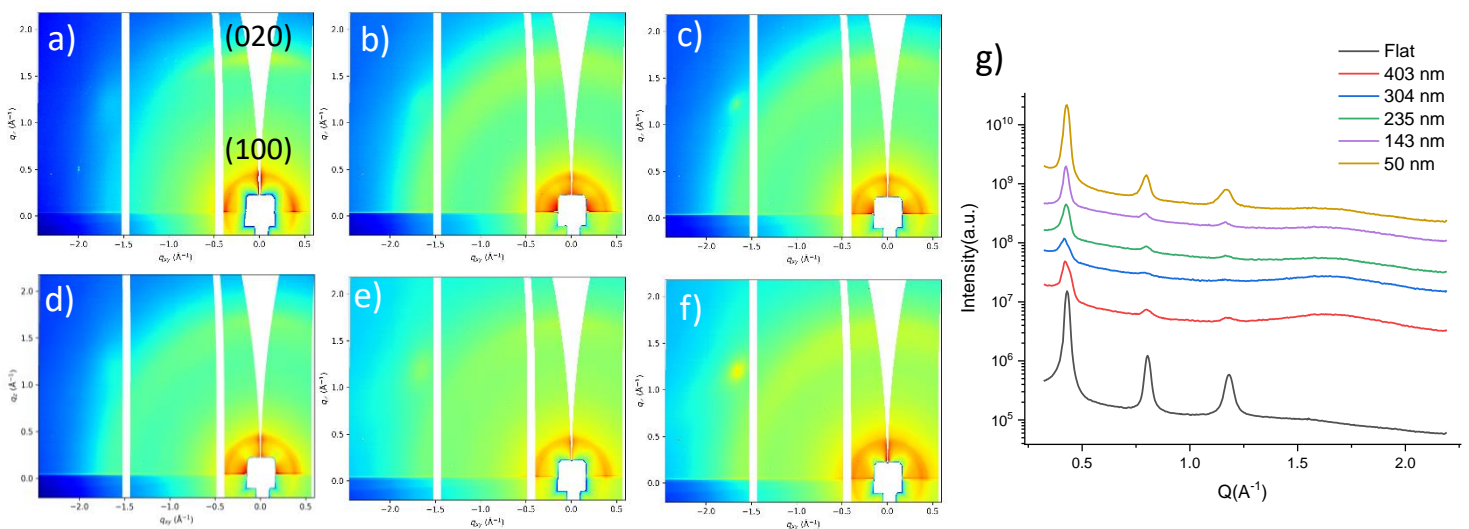


**Figure 1.** 2D GID pattern of P3HT out of equilibrium on flat substrate (a) and on substrates having different particles diameter 403nm (b), 304 (c), 235 nm (d), 143nm (e) and 50 nm (f). **Fig.1g:** Out of plane diffractogram of P3HT after *ex-situ* thermal annealing on flat substrate and on substrates having different particles diameter ranging from 403nm to 50nm.

As-prepared samples showed the expected low degree of crystallinity. However, although the  $\langle 100 \rangle$  diffraction signal appeared always as a ring, on the flat substrate higher intensity is observed along  $q_z$  and  $q_{xy}$  direction respectively, see Fig. 1 a, suggesting that crystals predominantly adopt the two well known orientation, edge-on and face-on. On the other hand, on nano-curved substrates, the intensity of  $\langle 100 \rangle$  peak is homogenous along the whole ring (see Fig. 1b-f). This suggests that crystal deposition spin-coating, although leading to random

orientations, can be viewed as a “dice rolling”. In other words, the few crystals formed during the fast solvent evaporation tend to stick to the substrates by adhesion of one of the crystalline faces. This leads, in the case of the flat substrates, to the presence of two main crystal orientations having, respectively, the polymer backbone parallel (edge-on) or perpendicular (flat-on) to the substrate plane. On the other hand, on nano-curved substrates, the adhesion of the crystal faces on the curved portions of nano-curved substrates leads to an isotropic orientation of the polymer backbone with respect to the substrate plane. This homogeneous distribution of crystals is expected to be responsible for the observed higher electrical conductivity of polymer films deposited on nano-curved substrates which we reported in the proposal of the present experiment. Upon thermal-annealing, P3HT is known to adopt almost exclusively the edge-on orientation, that is, the polymer backbone is laying parallel to the substrate plane, as confirmed by the high  $\langle 100 \rangle$  peak intensity along the  $q_z$  direction for samples deposited on flat substrates (see Fig. 1.g. (black plot)). Vice-versa, on nano-curved substrates the conformal adhesion of polymer lamellae to particles leads to both edge-on and flat-on orientation, as revealed by the simultaneous presence of  $\langle 100 \rangle$  and  $\langle 020 \rangle$  peaks along the  $q_z$  direction (see Fig. 1.g). Indeed, due to the curvature, the same lamella gives rise to both edge-on orientation, from the portion laying on the top of particles, and to flat-on one from the portion adhering to the equatorial region of particles. The in-situ structural characterization was employed to determine other differences which may appear between flat and nano-curved substrates during thermal annealing. In particular, as the crystal growth on curved substrates is expected to induce structural distortion and, as a consequence, lower crystallization enthalpies, we monitored, during cooling, the temperature at which Bragg peaks appear.

As a matter of fact, on flat substrates the peak appeared at  $200^\circ\text{C}$  (see Fig. 2a), in agreement with what observed previously in literature, while on nano-curved ones the crystallization temperatures are lower (see Fig. 2b), ranging between  $170$  and  $150^\circ\text{C}$ . Although the limited experimental time, accentuated by the remote mode which prevented us to entirely exploit the 24 hours of a day, did not allow the study of the comprehensive effect of the nano-curvature, that is of the particle diameter, on the crystallization temperature lowering, our results unambiguously show that P3HT crystals grown on nano-curved substrates are clearly distorted and that this distortion reflects on a lower crystallization temperature.

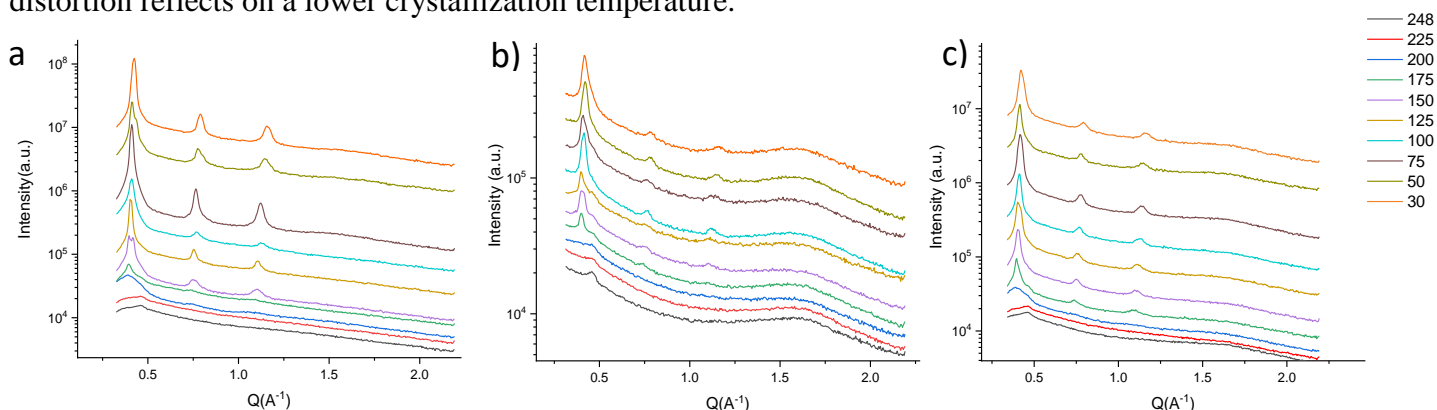


**Figure 2.** Comparison between out of plane diffractogram of P3HT in-situ thermal annealing on substrates having different curvature and SFE: flat substrate (a) and substrate with particles diameter of  $235\text{nm}$ (b), both with SFE of  $63.98\text{ mN/m}$ , while c shows the substrate having particles diameter of  $143\text{nm}$  and SFE of  $43.56\text{mN/m}$ .

Finally, in order to investigate the combined effect of nano-curvature and SFE on the P3HT crystallization, we performed the in-situ GID characterization on substrates characterized by constant nano-curvature but different SFE ( $63.98$ ,  $55.49$  and  $43.56\text{ mN/m}$  respectively). At the lowest SFE (Fig.2.c), the  $\langle 100 \rangle$  Bragg peak appears at  $200^\circ\text{C}$  again, suggesting dewetting from the low SFE curved portion of the substrates and growth of undistorted crystals taking place exclusively in the interstices between them.

By increasing the SFE, the Bragg peak  $\langle 100 \rangle$  appears at a lower temperature, which suggests the crystal growth not only in the interstices between the particles but also in the curved portion, resulting in the formation of distorted crystals. The above implies the presence of an energy gain that balances the loss of crystallization enthalpy resulting from the growth of distorted crystals.

In order to verify the hypothesis of the change from the full retraction to full wetting with the increase of SFE, the analysis of GISAXS data is currently ongoing, as the dewetting is expected to increase the contrast of the nanoparticles monolayer form factor.